# Effect of Anion in Diluted Imidazolium-based Ionic Liquid/Buffer Electrolytes for CO<sub>2</sub> Electroreduction on Copper

Samaneh Sharifi Golru <sup>a,b</sup>, Elizabeth J. Biddinger <sup>a,b,\*</sup>

<sup>a</sup> Department of Chemical Engineering, The City College of New York, CUNY, New York, NY 10031, USA

<sup>b</sup> Ph.D. Program in Chemistry, The Graduate Center of City University of New York, CUNY,
New York, NY 10016, USA

\*Corresponding author. Tel.: +1 212 650 6323; fax: +1 212 650 6666.

E-mail address: <a href="mailto:ebiddinger@ccny.cuny.edu">ebiddinger@ccny.cuny.edu</a>

**Abstract** 

A series of ILs containing the same cation (1-butyl-3-methylimidazolium ([BMIM]<sup>+</sup>)) but

different anions (bis(trifluoromethylsulfonyl)imide ([NTF<sub>2</sub>]<sup>-</sup>), triflate ([OTF]<sup>-</sup>), acetate ([Ac]<sup>-</sup>),

chloride ([Cl]-), and dicyanamide ([DCA]-)) were used to study the effect of anion in diluted

imidazolium-based ionic liquid/buffer electrolytes on product selectivity and activity of copper

electrodes in CO<sub>2</sub> electroreduction. The onset potential shifted to more positive potentials by

adding ILs to the CO<sub>2</sub>-saturated electrolytes. Faradaic efficiency (FE%) of formate for all ILs

(except for [BMIM][DCA]) increased compared to the electrolyte without any IL at all potentials.

The maximum FE<sub>formate</sub> (38.7%) was observed for [BMIM][NTF<sub>2</sub>] at -0.92 V. [BMIM][DCA] had

the highest FE% for hydrogen and the lowest FE% for hydrocarbons. By using X-ray photoelectron

spectroscopy, the maximum amount of IL adsorbed on the surface was obtained for

[BMIM][DCA] which had the highest hydrophilicity and lowest CO<sub>2</sub> affinity. These results

underscore the importance of anions when using ILs for CO<sub>2</sub> electroreduction.

Keywords: CO<sub>2</sub> reduction, Cu electrodes, Ionic liquids, Electrocatalysis.

2

#### 1. Introduction

Although carbon dioxide (CO<sub>2</sub>) as a greenhouse gas has created serious problems in the atmosphere such as global warming and climate change, it can be considered as a carbon source to produce valuable chemicals and fuels[1]. Electroreduction of CO<sub>2</sub> (CO2ER), as one of the promising methods for carbon dioxide utilization, has attracted much attention[2]. Challenges for CO2ER include the high overpotential needed to reduce the linear CO<sub>2</sub> molecule[1] and, the presence of parasitic hydrogen evolution reaction (HER) that suppress the formation of the desired products in CO2ER[2]. Cu has been reported to have a potential to electrochemically convert CO<sub>2</sub> to hydrocarbons and oxygenates[3], however, a mixture of products is formed on Cu catalysts[1, 3]. Thus, there is a need to make a more selective system. The selectivity and efficiency can be improved by controlling the design of the reaction system (catalyst, electrolyte or reactor)[4-13]. From the electrolyte view, the electrolyte composition, water content and solution pH play key roles in CO2ELR[9-23].

Ionic liquids (ILs) have recently attracted the attention of researchers in the field due to their unique properties such as the high CO<sub>2</sub> absorption capacity[9, 11, 12, 22-30]. In one of the first reports for using ILs in CO2ER, Rosen et al. showed the production of CO from CO<sub>2</sub> electroreduction in a mixture of 1-ethyl-3-methylimidazolium tetrafluoroborate ([EMIM][BF4]) and water (18% IL) with a high faradic efficiency and low overpotential on a silver cathode[26]. Zhou et al. also found that ILs with chloride ions such as 1-butyl-3-methylimidazolium chloride ([BMIM][Cl]) could be an efficient candidate for CO<sub>2</sub> reduction to CO and HER inhibition[31]. They attributed this observation to the interactions of ions with water in the electrolyte (80% IL in water) [31].

Depending on many factors such as type of catalyst and IL, the main product in CO2ER can vary in IL-added electrolytes. One of the products which can be produced with high faradaic efficiencies in ILs in CO<sub>2</sub> electroreduction is formate[28]. Formate has many applications such as an H<sub>2</sub> and syngas storage material, and in direct formic acid fuel cells[28, 32]. Huan et al. reported that a dendritic Cu catalyst with high surface area produced 80% formic acid in 1-ethyl-3-methylimidazolium tetrafluoroborate, ([EMIM][BF4]) /water mixture (92% IL) [28].

It has been hypothesized that ILs can activate CO<sub>2</sub> molecules[9], stabilize the catalytic intermediates and consequently decrease the energy barrier and overpotential in CO2ER [23, 26, 28]. In ILs, the linear structure of CO<sub>2</sub> is distorted due to the interaction of IL-CO<sub>2</sub> [27]. This effect can lower the CO2ER overpotential[27]. The properties of ILs are affected by several parameters such as the nature and size of ions, functional groups, temperature, and pressure[33-38]. Depending upon the structural properties, the ILs demonstrate different interactions with the metal surface and consequently, alter the double layer thickness[39-43]. A recent computational study on using the hydrophobic and hydrophilic imidazolium-based ILs containing the same cation, [BMIM]<sup>+</sup>, but various anions (Cl<sup>-</sup>, [DCA]<sup>-</sup>, [HCOO]<sup>-</sup>, [BF4]<sup>-</sup>, [PF6]<sup>-</sup>, [CH<sub>3</sub>SO<sub>3</sub>]<sup>-</sup>, [OTF]<sup>-</sup>, and [NTF<sub>2</sub>]<sup>-</sup>) on Au surface showed that anions significantly affect the adsorption of an IL on the surface[39]. They also reported that the electrostatic interactions a long with van der Waals forces interactions play key roles in IL adsorption on metals[39].

Although ionic liquids have been previously used in many studies to enhance CO<sub>2</sub> electroreduction on various metals, most of the research, to our knowledge, have focused on high concentrated electrolytes. Also, Cu has been less studied for CO2ER in IL-based electrolytes. In this work, we report the influence of low concentrations of imidazolium-based ILs in aqueous

bicarbonate electrolytes on the selectivity and activity of Cu catalysts in CO2ER. Using diluted IL electrolytes allowed us to avoid any mass transfer limitations due to increased viscosity and reduced conductivity, and provide sufficient protons to produce hydrogen-rich products. In this research, we focus on the effect of anion nature in CO2ER. Hence, a series of ionic liquids containing the same cation (1-butyl-3-methylimidazolium ([BMIM]<sup>+</sup>)) and various anions: bis(trifluoromethylsulfonyl)imide ([NTF<sub>2</sub>]<sup>-</sup>), triflate ([OTF]<sup>-</sup>), acetate ([Ac]<sup>-</sup>), chloride ([Cl]<sup>-</sup>), and dicyanamide ([DCA]) were used. The imidazolium cation was used because it has been reported to lower the energy barrier for CO<sub>2</sub> reduction by creating a complex with CO<sub>2</sub>[23, 26, 28]. The anions were chosen to cover different hydrophilicity, size, and CO<sub>2</sub> affinity. [NTF<sub>2</sub>] is considered as a hydrophobic anion, [OTF] has a medium hydrophobicity, and [Ac], [Cl], and [DCA] are considered as hydrophilic anions[33, 39]. The size of the anion also increases with the following order:  $[C1]^- < [Ac]^- < [DCA]^- < [OTF]^- < [NTF_2]^- [44]$ . One of the important parameters in ILs which is mainly determined by the anion is CO<sub>2</sub> affinity[44-52]. The CO<sub>2</sub> solubilities for the ILs studied differ because of their basicity[48-50], molar volume[50, 52], and the number of fluorine groups [44, 47, 51]. The CO<sub>2</sub> absorption capacity of [BMIM]<sup>+</sup> ILs are in the following order: [Cl]<sup>-</sup> < [DCA]<sup>-</sup><< [OTF]<sup>-</sup> < [NTF<sub>2</sub>]<sup>-</sup> << [Ac]<sup>-</sup> at 25 °C [44, 47-49, 53]. [Ac]<sup>-</sup> -based ILs have a much higher CO<sub>2</sub> solubility compared to other ILs due to the high basicity of [Ac] which causes the IL to chemically react with CO<sub>2</sub> [54]. Among the ILs interacting physically with CO<sub>2</sub>, [NTF<sub>2</sub>] has the maximum CO<sub>2</sub> affinity due to its large molar volume and the number of fluorine atoms in the anion[44, 47, 50-52]. Although it is unlikely that changing the anion in our diluted IL/buffer mixtures affect the CO<sub>2</sub> solubility in the bulk electrolyte, it may alter the local CO<sub>2</sub> concentration at the surface. Moreover, the ILs used in this study had similar cathodic limits in the electrochemical potential window [55], indicating electrochemical degradation of the IL is not likely to be a differentiating factor in this study.

#### 2. Experimental

## 2.1. Electrode preparation

Polycrystalline Cu flags with 0.9 cm<sup>2</sup> geometric area were used in this work. To make the Cu flags, a  $0.5 \times 0.7 \times 0.01$  cm<sup>3</sup> Cu foil was connected to a 1.25 cm of a twisted Cu wire with 0.5 mm diameter. Both Cu foils and wires had 99.999% purity and were purchased from Alfa Aesar. The electropolishing process was first performed on Cu electrodes in 1 M phosphoric acid (H<sub>3</sub>PO<sub>4</sub>) at 1.8 V for 300 s to create a relatively smooth surface. The electropolishing process allows us to eliminate any catalyst morphological effect and just focus on the electrolyte impact in CO<sub>2</sub> electroreduction in this work.

#### 2.2. Electrochemical analysis

An H-type cell with a Nafion-212 membrane to separate the cathodic and anodic compartments (Figure S1) was used for all electrochemical experiments including cyclic voltammetry, electrochemical impedance spectroscopy, and the CO<sub>2</sub> electroreduction experiments. The anolyte was 0.1 M potassium bicarbonate (KHCO<sub>3</sub>, Fisher Chemical, Certified ACS) and the catholyte was a solution of 0.1 M KHCO<sub>3</sub> and 10 mM of an IL. All studied ILs had the same cation, 1-butyl-3-methylimidazolium ([BMIM]<sup>+</sup>), with various anions: bis(trifluoromethylsulfonyl)imide ([NTF<sub>2</sub>]<sup>-</sup>), triflate ([OTF]<sup>-</sup>), dicyanamide ([DCA]<sup>-</sup>), acetate ([Ac]<sup>-</sup>), and chloride ([Cl]<sup>-</sup>). All ILs were purchased from Ionic Liquid Technologies (Io-Li-Tec) Inc. Before adding the ILs to the

electrolyte, pretreatment of the buffer solution (0.1 M KHCO<sub>3</sub>) was performed overnight at -0.0125 mA to remove any impurities from the electrolyte [5, 56]. The electrochemical experiments were carried out by a Gamry Interface 1000 potentiostat. The reference and counter electrode were an Ag/AgCl electrode (BASi) and a Pt-mesh, respectively. To convert the potentials from Ag/AgCl (3 M NaCl) to reversible hydrogen electrode (RHE) the equation  $V_{vs.\,RHE} = V_{measuredvs.Ag/AgCl} + 0.209 +0.059 \, pH_{solution}$  was used. In order to compensate for the IR drop due to the electrolyte resistance, current-interrupt method was used. All measurements were repeated at least three times to evaluate the repeatability.

## 2.2.1. Cyclic voltammetry (CV)

Prior to the electrochemical CO<sub>2</sub> reduction reaction, the cyclic voltammetry (CV) experiments were performed in the potential range from -1.0 V to -1.8 V vs. Ag/AgCl with a 50 mV/s scan rate in N<sub>2</sub>- and CO<sub>2</sub>-saturated electrolytes. To saturate the electrolyte for each experiment, the gas was bubbled to the catholyte for 30 mins before each experiment. Regardless of IL type, the pH values of N<sub>2</sub>-saturated and CO<sub>2</sub>-saturated electrolytes were 9.3 and 6.8, respectively.

## 2.2.2. Electrochemical Impedance Spectroscopy (EIS)

The electrochemical impedance spectroscopy (EIS) was also performed in CO<sub>2</sub>-saturated electrolytes to measure the cell and charge transfer resistance in different electrolytes before CO<sub>2</sub> reduction experiments. The EIS analysis was performed in the frequency range of 10 KHz to 0.1 Hz at -0.92 V and -1.12 V versus RHE. The AC amplitude was 10 mV. Figure S2 and Table S1 shows the equivalent circuits and the parameter values after fitting the EIS data.

## 2.2.3. CO<sub>2</sub> electroreduction (CO2ER)

After CVs and EIS, a pre-CO<sub>2</sub> electroreduction experiment was carried out at -1.02 V for 30 mins in CO<sub>2</sub>-saturated electrolyte. This pre-electrolysis experiment allows the surface oxides to get reduced to the pure Cu. Before each experiment, the electrolyte was saturated by carbon dioxide gas (Praxair, purity 99.99 %) for 30 mins. The CO<sub>2</sub> flow rate was 35 ml/min for all experiments. CO<sub>2</sub> electroreduction was performed at different potentials (-0.92 V, -1.02 V, -1.12 V, and -1.19 V vs. RHE) for 30 mins. Micro GC and <sup>1</sup>H NMR were used to detect and quantify the gaseous and liquid products, respectively. More experimental details can be found in the Supporting Information. <sup>1</sup>H NMR spectra after CO2ER at -0.92 V in different electrolytes were provided in Figure S3.

#### 2.3. Conductivity measurement

Conductivity for all studied electrolytes was obtained using electrochemical impedance spectroscopy measurements (EIS). The electrochemical cell for the conductivity measurement was a 1ml class A volumetric flask with two platinum wires (0.762 mm diameter, 99.95%, Alfa Aesar). The solution resistance was first measured by doing EIS at the frequency range of 100 Hz – 100 kHz at 5 mV. The impedance at the highest frequency is the solution resistance. Then, Eq.1 can be used to find the conductivity.

$$\sigma = C/R$$
 Eq.1

Where  $\sigma$ , R, and C are conductivity, solution resistance, and cell constant, respectively. Using a standard solution of 0.010M potassium chloride (KCl, from Ricca Chemical) whose conductivity was known as 1412  $\mu$ S/cm cm at 25 °C, the cell constant was first obtained (0.592  $\pm$  0.017 cm<sup>-1</sup>). The conductivity values for the electrolytes were provided in Figure S4.

# 2.4. X-ray photoelectron spectroscopy (XPS)

In order to analyze the electrode surface after CO<sub>2</sub> electroreduction in IL-free and IL-added electrolytes, XPS was used. To prepare the samples for XPS, the electrodes were first rinsed with DI water and then were dried at 40 °C in vacuum oven overnight. The XPS measurements were performed with a Physical Electronics PHI 5000 VersaProbe II spectrometer using a monochromatic Al Kα radiation (1486. 6 eV, 50 W, 15 kV). The operating pressure was 10<sup>-8</sup> Torr. Multipack and XPSPEAK softwares were used to analyze and fit the spectra. The binding energies were normalized to C 1s peak (284.8 eV) for all spectra.

#### 3. Results and discussion

Prior to CO<sub>2</sub> electroreduction experiments, cyclic voltammetry measurements in N<sub>2</sub>- and CO<sub>2</sub>-saturated electrolytes were performed to evaluate the initial HER (Figure 1a-e) and CO2ER + HER (Figure 1f-j) activity of the Cu electrodes in different ILs. According to Figure 1a-e, the HER current density for all ILs (except [BMIM][DCA]) was lower compared to IL-free electrolyte. This observation is most notable for [BMIM][Ac], where the current density was decreased by 34.6% at -1.0 V. However, [BMIM][DCA] (Figure 1e) showed a much higher current density in N<sub>2</sub>-saturated electrolytes compared to IL-free electrolyte. For instance, the current density in N<sub>2</sub>-saturated electrolyte increased by 165.8% at -0.9V by adding 10 mM [BMIM][DCA]. This observation is likely attributed to its high hydrophilic nature which cause more water molecules to adsorb on the surface.

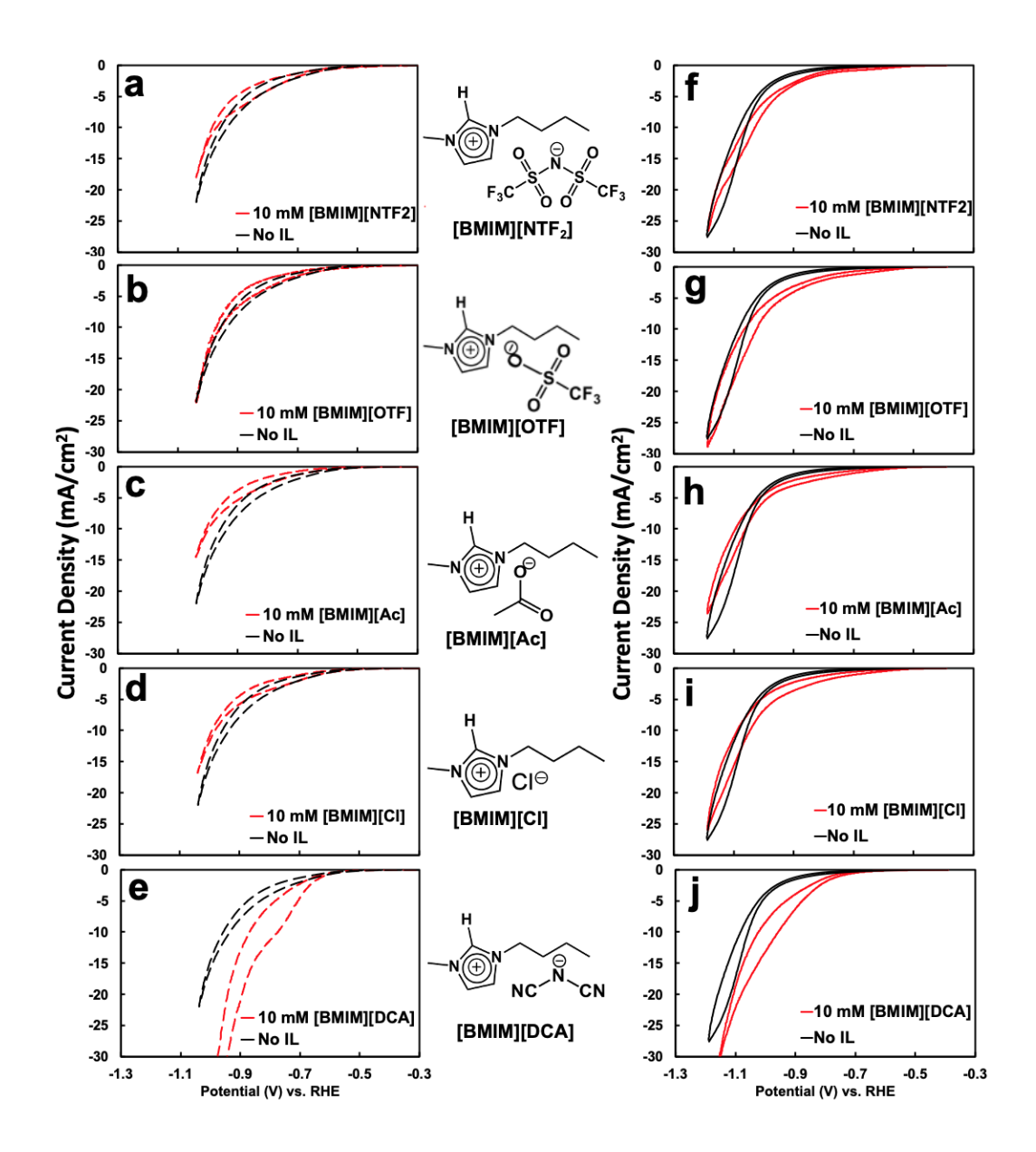


**Figure 1.** Comparison of the CVs for HER (a-e) and CO2ER (f-j) on Cu in IL-free and IL-added 0.1 M KHCO<sub>3</sub> electrolyte. The electrolyte was saturated with N<sub>2</sub> (a-e) and CO<sub>2</sub> (f-j) for 30 mins before CVs measurements.

A comparison of the CV curves in CO<sub>2</sub>-saturated electrolytes (Figure 1f-j) showed that the onset potential in the presence of CO<sub>2</sub> shifted to a more positive potential by adding IL to the electrolyte. In particular, [BMIM][Ac] showed a +0.20 V shift compared to IL-free electrolyte. This observation shows the higher activity of the surface in IL-added electrolytes. Moreover, it was observed that the current density for IL-added electrolytes was higher compared to IL-free electrolyte at more positive potentials. However, a lower or similar current density for IL-added

electrolytes (except [BMIM][DCA]) compared to IL-free electrolytes was observed at more negative potentials. For example, the current density for [BMIM][Ac] was higher than IL-free electrolyte from -0.58 V to -1.05 V, while after -1.05 from, [BMIM][Ac] had a lower current density compared to when the IL was absent. The current density for [BMIM][DCA] was higher than IL-free electrolyte at all potentials studied.

ILs affected the structure of the double layer at the interface differently depending on the IL configurations and other properties. Diffusion of the reactants such as CO<sub>2</sub> and water molecules, and also the stability of the intermediates at the electrode surface are impacted by the structure of the double layer. EIS were used to evaluate the interface at -0.92 V and -1.12 V in CO<sub>2</sub>-saturated electrolytes.

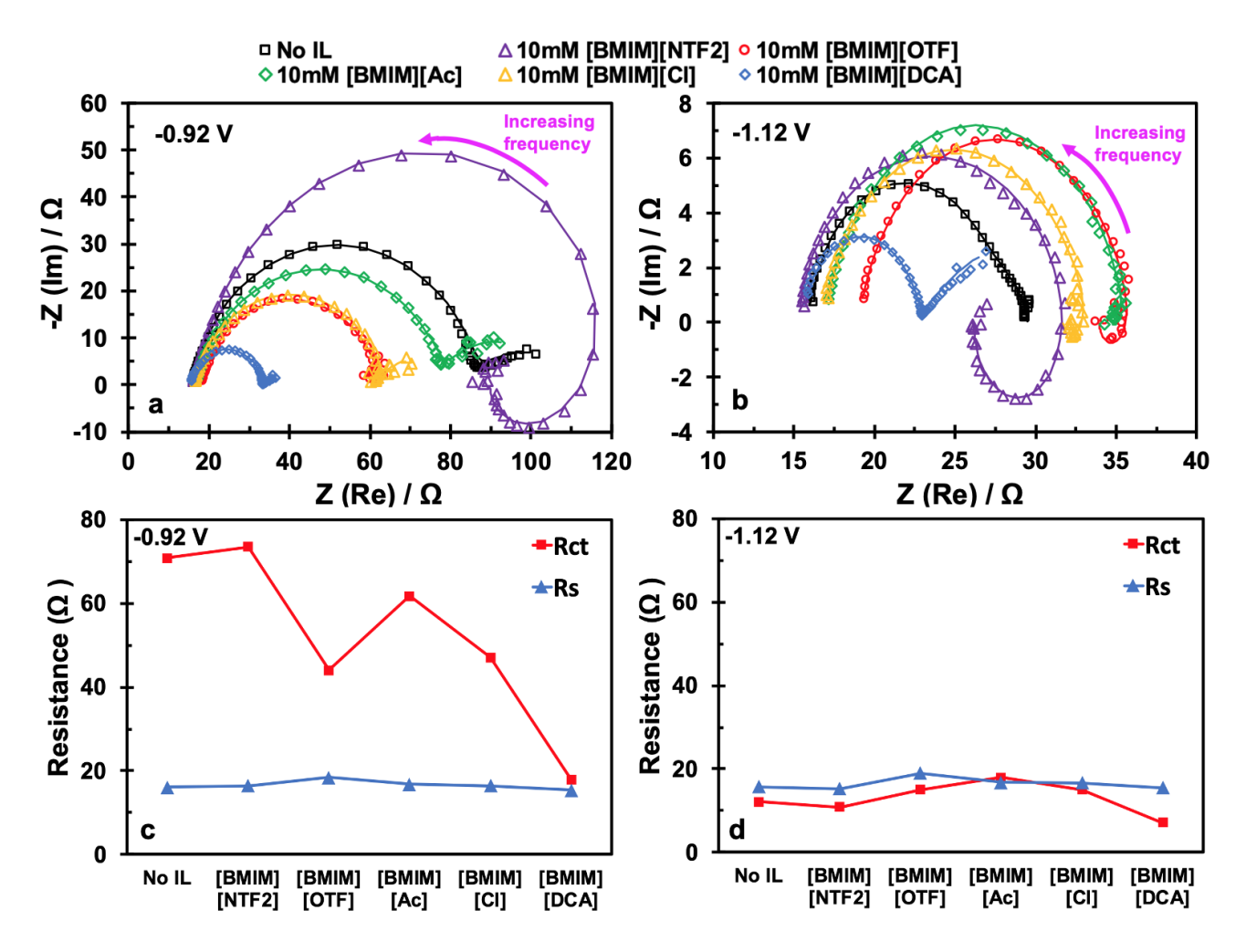


**Figure 2.** (a-b), Nyquist plots (c-d) solution and charge transfer resistance for the CO<sub>2</sub>-saturated electrolytes at -0.92 V and -1.12 V. Solid lines in a and b are the fitted curves according to the equivalent circuits in Fig. S2.

Figure 2a-b shows the Nyquist plots for CO<sub>2</sub>-saturated 10 mM IL-containing and IL-free electrolytes at -0.92 and -1.12 V. Two equivalent electric circuits (Figure S2) were used to fit the data and parameters are provided in Table S1. The equivalent circuits simulated using the EIS data showed that the electrochemical system consisted of three resistances, two pseudo-capacitances, with or without one inductance, as shown in Figure S2. In the equivalent circuits, R<sub>s</sub> is the bulk solution resistance, CPE<sub>dl</sub> is the double-layer pseudo-capacitance, R<sub>ct</sub> is the charge-transfer resistance associated with the double layer, R<sub>1</sub> and CPE<sub>1</sub> can be the resistance and pseudo-

capacitance related to the adsorbed intermediates on the surface, respectively[29, 57]. L is also an inductor attributed to the dynamic adsorption/desorption of ionic liquids on the surface[58]. Different R<sub>ct</sub> values for the electrolytes indicate the unique behavior of each IL at the surface. According to Figure 2 and Table S1, R<sub>ct</sub> for each electrolyte was significantly impacted by the potential; However, the R<sub>s</sub> (intercept on the x-axis at high frequency on the Nyquist plot) did not noticeably change by the potential (scales used on Figures 2a and b are different for ease of reading results). R<sub>s</sub> usually depends on the electrode geometry and size, the distance between the electrodes, temperature, type of ions and also the electrolyte conductivity[59]. The results from the conductivity measurements (Figure S4) also showed the electrolytes had similar conductivity values in the range of 9600-10300 mS/cm which is in agreement with similar R<sub>s</sub> obtained for the electrolytes.

A number of parameters were found to be potential dependent from the EIS examination. At the most positive potential (-0.92 V), all IL electrolytes except [BMIM][NTF2] followed a similar behavior. Therefore, we used the equivalent circuit 1 (Figure S2) to fit the Nyquist data for all IL electrolytes except [BMIM][NTF2] at -0.92 V. All ILs except [BMIM][NTF2] showed a lower  $R_{et}$  compared to IL-free electrolyte at -0.92 V (Table S1). For example, IL free electrolyte had 70.8  $\Omega$  while [BMIM][NTF2], [BMIM][OTF], [BMIM][Ac], [BMIM][C1], and [BMIM][DCA] had 73.5, 44.0, 61.7, 47.0, and 18.0  $\Omega$  charge transfer resistance, respectively. The lower  $R_{et}$  is indicative of higher rate of ion transfer (higher current density) for the electrolytes. Among ILs, a different behavior was observed for [BMIM][NTF2] at -0.92 V. [BMIM][NTF2] showed an inductive loop at low frequency. The low frequency inductive loop can be associated to the adsorption/desorption of the species at the surface[58]. This can be indicative of the weak interaction of [BMIM][NTF2] with Cu surface. It has been previously reported that the hydrophobic anions have weak

interactions with the metal surface[39, 40]. The high R<sub>ct</sub> for [BMIM][NTF<sub>2</sub>] is likely due to the large size of this ILs which can complicate the charge transfer on the surface.

At a more negative potential (-1.12 V), a different behavior was observed for the ILs compared to -0.92 V. Although increasing the overpotential did not significantly affect the R<sub>s</sub>, lower charge transfer resistance (R<sub>ct</sub>) was observed for all electrolytes at the more negative potential of -1.12 V. This observation is attributed to the easier electron transfer at higher overpotentials due to the lower energy barrier for the reactions. All ILs except [BMIM][DCA] and [BMIM][NTF<sub>2</sub>] had a higher R<sub>ct</sub> compared to IL-free electrolyte, which is opposite of what was observed at -0.92V. Having a high R<sub>ct</sub> is likely attributed to the accumulation of the IL at the surface at negative potentials[60] which can block the CO<sub>2</sub> diffusion toward the surface. Similar to the potential of -0.92V, [BMIM][DCA] had the lowest R<sub>ct</sub> (7.53 Ω) among the other electrolytes at -1.02V. Moreover, an inductive loop at low frequency was observed at -1.12 V for all ILs except [BMIM][DCA]. As mentioned before, the presence of an inductive loop is associated with the dynamic adsorption/desorption of the species on the surface[58].

CVs and EIS allow for the examination of the total activity of CO2ER and HER combined. The product selectivity is key to provide a deeper understanding on the effect of ILs in CO2ER. Therefore, another important parameter, Faradaic efficiency (FE) is used to show the selectivity of the system toward CO2ER and HER. Faradaic efficiency is defined as the ratio of the charge consumed to produce a desired product to the total charge input into the system. In order to evaluate the product selectivity of the Cu catalyst in IL/KHCO3 mixtures, CO2 electroreduction experiments were carried out at different potentials (-0.92 V, -1.02 V, -1.12 V, and -1.19 V) for 30 mins on electropolished copper electrodes which were previously used in CVs and EIS experiments. By doing CVs before CO2ER experiments, most of copper oxides on the surface are reduced to Cu

metal. FE for the gaseous and liquid products produced during CO2ER are shown in Figure 3 (ad). Figure 3 shows that adding a small amount of ILs (10 mM) to the electrolytes had a significant impact on the product selectivity. All IL-containing electrolytes showed a higher FE for formate compared to IL-free electrolyte. The maximum increase (a 329% increase compared to IL-free electrolyte) in formate FE was obtained for [BMIM][NTF2] at -0.92 V. This observation may be due to the high CO<sub>2</sub> affinity and low hydrophilicity of [BMIM][NTF<sub>2</sub>]. By increasing the potential, the FE% for hydrocarbons and alcohol increased for all electrolytes which indicate the higher barrier energies for formation of these products compared to CO and formate[61, 62]. [BMIM][DCA] was the only IL that suppressed CO2ER and had the maximum FE% for H<sub>2</sub> at all studied potentials. This observation can be attributed to the high hydrophilicity and low CO<sub>2</sub> adsorption capacity of the [BMIM][DCA][63] at the surface leading to water molecules attraction and CO<sub>2</sub> molecules repulsion. Previous experimental and theoretical studies have been also reported high concentrations of water at the surface in [EMIM][DCA] /water mixtures[64, 65]. Accumulation of water molecules at the surface can be a reason to enhance HER[64]. There were also no C<sub>2</sub> products for [BMIM][DCA] even at higher overpotentials. For all ILs except [BMIM][Ac], the FE% toward C2 products decreased. The low FE% for C2 products in IL-added electrolytes can be due to the presence of [BMIM]<sup>+</sup>- CO<sub>2</sub><sup>-o</sup> complexes on the surface which can prevent CO<sub>2</sub> dimerization required for the formation of C<sub>2</sub> products. It was also previously reported that the presence of [EMIM]<sup>+</sup> cations on the surface hinders the interactions of CO<sub>2</sub> molecules with each other and blocks dimerization[66]. [BMIM][Ac] had the maximum FE% for C<sub>2</sub> products at -1.12V (a 27% increase in FE<sub>C2</sub>% compared to IL-free electrolyte). The [BMIM][Ac] had also the maximum FE% for CO at all potentials compared to all electrolytes. For example, [BMIM][Ac] had 19.9% FEco when IL-free electrolyte had 6.4 % FEco at -1.02V. It has been reported that [Ac]

-based ILs can make chemical interactions with CO<sub>2</sub> because of the high basicity of the [Ac] anions while the interaction of other ILs with CO<sub>2</sub> molecules is mostly physical[54]. The reaction pathway for CO and C<sub>2</sub> products are different from the formate formation pathway, [67], and the [BMIM][Ac] chemical interaction with CO<sub>2</sub> seems to promote the CO pathway. The total FEs% obtained for IL-free and IL-added electrolytes were provided in Figure S5.

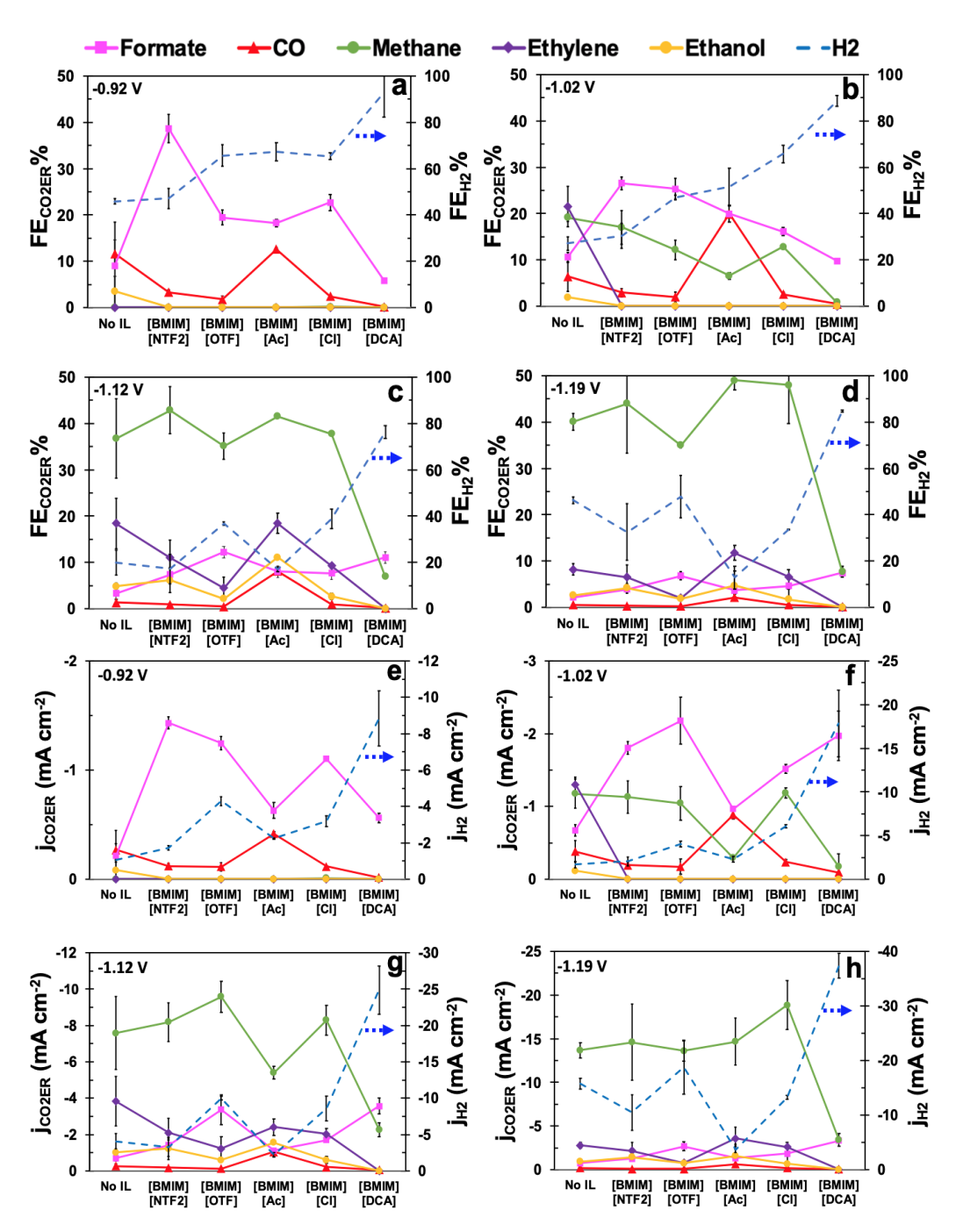


**Figure 3.** Faradaic efficiency (a-d) and partial current density (e-h) of the main products produced in 10 mM IL/KHCO<sub>3</sub> electrolytes at different potentials (left and right vertical axes for each chart correspond to the products produced in CO2ER and HER reactions, respectively).

Another important parameter in CO2ER is partial current density for each product which shows the average activity of the catalyst for each reaction in 30 mins CO2ER. The partial current density is the proportion of the total current density that goes for a desired product. As it can be seen in Figure 3 (e-h), ILs also significantly affected the partial current density. The total current density for CO<sub>2</sub> reduction reactions at -0.92 V increased by adding ILs to the electrolyte. This can be justified by the presence of the ILs at the surface which stabilize CO<sub>2</sub>. intermediates on the surface and enhance CO2ER[28]. The formate current densities for all ILs at all potentials were also higher than that in IL-free electrolyte. The total current density (both CO2ER and HER) during 30 mins CO2ER at -0.92 V and -1.12 V are also provided in Figure S6.

In order to study the surface chemical change due to CO2ER in ILs, XPS was performed after CO2ER. The results for XPS showed the adsorption of ILs on the Cu surface during electrolysis (Figure S7, S8, and Table S2). The spectrum for the Cu electrode used in IL-free electrolyte had only C, O, and Cu. However, for the Cu electrodes used in all IL-added electrolytes, N was also detected on the surface (Figure S7 and S8). This illustrates the strong interaction of the IL with the surface. [BMIM][DCA] had a much higher amount of N on the surface (4.6 at%) compared to other ILs. Even after normalization the high N content of [BMIM][DCA], a higher amount of IL was present on the surface in case of [BMIM][DCA] compared to other ILs. It was also reported in other studies that hydrophilic ILs can make a stronger interaction with metal surface compared to the hydrophobic ILs[39, 40]. In our research, no S, F, or Cl was detected on the surface for [BMIM][NTF2], [BMIM][OTF], and [BMIM][Cl], most likely due to concentrations below the detection limit of the instrument. The results showed that although IL adsorption is important to make the IL-CO2 complex on the surface, a strong IL adsorption can poison the surface, block the diffusion of CO2 to the surface, and consequently, suppress CO2ER.

#### 4. Conclusion

Herein, we demonstrated that a small amount of ionic liquids significantly affected the product selectivity and catalytic activity in CO<sub>2</sub> electroreduction on Cu. The performance of the ILs is highly dependent on the potential. The CVs and total current measurements during the electrolysis showed that IL added electrolytes had higher activity compared to IL-free electrolyte at the most positive potential (-0.92 V). However, at more negative potentials, the activity for the IL added were lower than that in IL-free electrolyte probably due to the accumulation of ILs at the surface and blocking the diffusion of CO<sub>2</sub> to the surface. The EIS also confirmed the fast reaction rate (low R<sub>ct</sub>) in ILs at the most positive potential (-0.92 V). Product selectivity was also significantly altered in the presence of ILs. By adding ILs to the electrolyte, the formate FE% increased (except [BMIM][DCA]). The maximum increase in formate FE% was observed for [BMIM][NTF<sub>2</sub>] at -0.92V which had the highest CO<sub>2</sub> affinity and lowest hydrophilicity. The XPS also showed the presence of the IL with the Cu surface after electrolysis indicating the strong interaction of IL with the surface especially for [BMIM][DCA]. Among ILs studied here, [BMIM][DCA] was the only IL which shut off the CO2ER and enhanced HER at all potentials probably because of the low CO2 affinity and high hydrophilicity at the surface. The results obtained in this work indicated that the nature of anion significantly affects CO2ER. Although the ILs are assumed to be the first layer adsorbed on the electrode surface, the diffusion of water molecules and finally the concentration of water on the surface are highly dependent on the nature of ILs. More hydrophilic anions can let more water molecules accumulate at the surface and consequently enhance HER. In contrast, bulky and hydrophobic ILs have a reduced amount of water and higher amount of CO<sub>2</sub> at the surface.

ASSOCIATED CONTENT

Supporting Information. The Supporting Information including XPS analysis, EIS, and

additional experimental details is available free of charge on the ACS Publications website at DOI:

**AUTHOR INFORMATION** 

Corresponding Author

\*E-mail: ebiddinger@ccny.cuny.edu

**ORCID** 

Samaneh Sharifi Golru: 0000-0002-0136-7555

Elizabeth J. Biddinger: 0000-0003-3616-1108

**Notes** 

The authors declare no competing financial interest.

Acknowledgments

The work is supported by National Science Foundation (Grant No. 1935957). The authors

would like to acknowledge the Surface Science and also Biomolecular NMR Facilities of CUNY

Advanced Science Research Center for instrument use. The NMR experimental help of Dr. James

Aramini is appreciated.

20

- [1] K.P. Kuhl, E.R. Cave, D.N. Abram, T.F. Jaramillo, New insights into the electrochemical reduction of carbon dioxide on metallic copper surfaces, Energy Environ. Sci., 5 (2012) 7050-7059.
- [2] O.G. Sánchez, Y.Y. Birdja, M. Bulut, J. Vaes, T. Breugelmans, D. Pant, Recent advances in industrial CO<sub>2</sub> electroreduction, Curr. Opin. Green Sustain. Chem., 16 (2019) 47-56.
- [3] Y. Hori, A. Murata, R. Takahashi, Formation of hydrocarbons in the electrochemical reduction of carbon dioxide at a copper electrode in aqueous solution, J. Chem. Soc., Faraday Trans. 1, 85 (1989) 2309-2326.
- [4] A.N. Karaiskakis, S. Sharifi Golru, E.J. Biddinger, Effect of electrode geometry on selectivity and activity in CO<sub>2</sub> electroreduction, Ind. Eng. Chem. Res., 58 (2019) 22506-22515.
- [5] A.N. Karaiskakis, E.J. Biddinger, Evaluation of the impact of surface reconstruction on rough electrodeposited copper-based catalysts for carbon dioxide electroreduction, Energy Technol., 5 (2017) 901-910.
- [6] W. Tang, A.A. Peterson, A.S. Varela, Z.P. Jovanov, L. Bech, W.J. Durand, S. Dahl, J.K. Norskov, I. Chorkendorff, The importance of surface morphology in controlling the selectivity of polycrystalline copper for CO<sub>2</sub> electroreduction, Phys. Chem. Chem. Phys., 14 (2012) 76-81.
- [7] M. Bernal, A. Bagger, F. Scholten, I. Sinev, A. Bergmann, M. Ahmadi, J. Rossmeisl, B.R. Cuenya, CO<sub>2</sub> electroreduction on copper-cobalt nanoparticles: size and composition effect, Nano Energy, 53 (2018) 27-36.
- [8] Z. Bitar, A. Fecant, E. Trela-Baudot, S. Chardon-Noblat, D. Pasquier, Electrocatalytic reduction of carbon dioxide on indium coated gas diffusion electrodes—Comparison with indium foil, Appl. Catal. B-Environ., 189 (2016) 172-180.

- [9] Y. Chen, T. Mu, Conversion of CO<sub>2</sub> to value-added products mediated by ionic liquids, Green Chem., 21 (2019) 2544-2574.
- [10] A.S. Varela, M. Kroschel, T. Reier, P. Strasser, Controlling the selectivity of CO<sub>2</sub> electroreduction on copper: The effect of the electrolyte concentration and the importance of the local pH, Catal. Today, 260 (2016) 8-13.
- [11] A.V. Rudnev, K. Kiran, A. Cedeño López, A. Dutta, I. Gjuroski, J. Furrer, P. Broekmann, Enhanced electrocatalytic CO formation from CO<sub>2</sub> on nanostructured silver foam electrodes in ionic liquid/water mixtures, Electrochim. Acta, 306 (2019) 245-253.
- [12] R.F. Zarandi, B. Rezaei, H.S. Ghaziaskar, A.A. Ensafi, Electrochemical reduction of CO<sub>2</sub> to ethanol using copper nanofoam electrode and 1-butyl-3-methyl-imidazolium bromide as the homogeneous co-catalyst, J. Environ. Chem. Eng., 7 (2019) 103141.
- [13] S. Verma, X. Lu, S. Ma, R.I. Masel, P.J.A. Kenis, The effect of electrolyte composition on the electroreduction of CO<sub>2</sub> to CO on Ag based gas diffusion electrodes, Phys. Chem. Chem. Phys., 18 (2016) 7075-7084.
- [14] J. Resasco, L.D. Chen, E. Clark, C. Tsai, C. Hahn, T.F. Jaramillo, K. Chan, A.T. Bell, Promoter effects of alkali metal cations on the electrochemical reduction of carbon dioxide, J. Am. Chem. Soc., 139 (2017) 11277-11287.
- [15] H. Zhong, K. Fujii, Y. Nakano, Effect of KHCO<sub>3</sub> concentration on electrochemical reduction of CO<sub>2</sub> on copper electrode, J. Electrochem. Soc., 164 (2017) F923-F927.
- [16] S. Kaneco, H. Katsumata, T. Suzuki, K. Ohta, Electrochemical reduction of CO<sub>2</sub> to methane at the Cu electrode in methanol with sodium supporting salts and its comparison with other alkaline salts, Energy Fuels, 20 (2006) 409-414.

- [17] P. Sebastian-Pascual, S. Mezzavilla, I.E.L. Stephens, M. Escudero-Escribano, Structure-sensitivity and electrolyte effects in CO<sub>2</sub> electroreduction: from model studies to applications, Chemcatchem, 11 (2019) 3624-3643.
- [18] M.R. Singh, Y. Kwon, Y. Lum, J.W. Ager, A.T. Bell, Hydrolysis of electrolyte cations enhances the electrochemical reduction of CO<sub>2</sub> over Ag and Cu, J. Am. Chem. Soc., 138 (2016) 13006-13012.
- [19] H. Hashiba, L.-C. Weng, Y. Chen, H.K. Sato, S. Yotsuhashi, C. Xiang, A.Z. Weber, Effects of electrolyte buffer capacity on surface reactant species and the reaction rate of CO<sub>2</sub> in electrochemical CO<sub>2</sub> reduction, J. Phys. Chem. C, 122 (2018) 3719-3726.
- [20] J. Resasco, Y. Lum, E. Clark, J.Z. Zeledon, A.T. Bell, Effects of anion identity and concentration on electrochemical reduction of CO<sub>2</sub>, ChemElectroChem, 5 (2018) 1064-1072.
- [21] V.J. Ovalle, M.M. Waegele, Understanding the impact of N-Arylpyridinium ions on the selectivity of CO<sub>2</sub> reduction at the Cu/electrolyte interface, J. Phys. Chem. C, 123 (2019) 24453-24460.
- [22] H.K. Lim, H. Kim, The mechanism of room-temperature ionic-liquid-based electrochemical CO<sub>2</sub> reduction: a review, Molecules, 22 (2017) 16.
- [23] A. Hailu, S.K. Shaw, Efficient electrocatalytic reduction of carbon dioxide in 1-ethyl-3-methylimidazolium trifluoromethanesulfonate and water mixtures, Energy Fuels, 32 (2018) 12695-12702.
- [24] S.S. Neubauer, R.K. Krause, B. Schmid, D.M. Guldi, G. Schmid, Overpotentials and faraday efficiencies in CO<sub>2</sub> electrocatalysis—the impact of 1-ethyl-3-methylimidazolium trifluoromethanesulfonate, Adv. Energy Mater., 6 (2016) 1502231-n/a.

- [25] J.T. Feaster, A.L. Jongerius, X.Y. Liu, M. Urushihara, S.A. Nitopi, C. Hahn, K. Chan, J.K. Norskov, T.F. Jaramillo, Understanding the influence of EMIM CI on the suppression of the hydrogen evolution reaction on transition metal electrodes, Langmuir, 33 (2017) 9464-9471.

  [26] B.A. Rosen, A. Salehi-Khojin, M.R. Thorson, W. Zhu, D.T. Whipple, P.J.A. Kenis, R.I. Masel, Ionic liquid-mediated selective conversion of CO<sub>2</sub> to CO at low overpotentials, Science, 334 (2011) 643-644.
- [27] N. Hollingsworth, S.F.R. Taylor, M.T. Galante, J. Jacquemin, C. Longo, K.B. Holt, N.H. de Leeuw, C. Hardacre, Reduction of carbon dioxide to formate at low overpotential using a superbase ionic liquid, Angew. Chem., Int. Ed., 54 (2015) 14164-14168.
- [28] T.N. Huan, P. Simon, G. Rousse, I. Génois, V. Artero, M. Fontecave, Porous dendritic copper: an electrocatalyst for highly selective CO<sub>2</sub> reduction to formate in water/ionic liquid electrolyte, Chem. Sci., 8 (2017) 742-747.
- [29] D.-w. Yang, Q.-y. Li, F.-x. Shen, Q. Wang, L. Li, N. Song, Y.-n. Dai, J. Shi, Electrochemical impedance studies of CO<sub>2</sub> reduction in ionic liquid/organic solvent electrolyte on Au electrode, Electrochimica Acta, 189 (2016) 32-37.
- [30] A. Kemna, N.G. Rey, B. Braunschweig, Mechanistic insights on CO<sub>2</sub> reduction reactions at platinum/ BMIM BF<sub>4</sub> interfaces from in operando spectroscopy, ACS Catal., 9 (2019) 6284-6292.
- [31] F. Zhou, S. Liu, B. Yang, P. Wang, A.S. Alshammari, Y. Deng, Highly selective electrocatalytic reduction of carbon dioxide to carbon monoxide on silver electrode with aqueous ionic liquids, Electrochem. Commun., 46 (2014) 103-106.
- [32] C. Rice, S. Ha, R.I. Masel, P. Waszczuk, A. Wieckowski, T. Barnard, Direct formic acid fuel cells, J. Power Sources, 111 (2002) 83-89.

- [33] A. Stark, K.R. Seddon, Ionic liquids, Kirk-Othmer Encyclopedia of Chemical Technology, John Wiley & Sons, Inc.2007, pp. 836-920.
- [34] A. Maiti, Theoretical screening of ionic liquid solvents for carbon capture, Chemsuschem, 2 (2009) 628-631.
- [35] M.M. Taib, T. Murugesan, Solubilities of CO<sub>2</sub> in aqueous solutions of ionic liquids (ILs) and monoethanolamine (MEA) at pressures from 100 to 1600 kPa, Chem. Eng. J., 181 (2012) 56-62.
- [36] M. Kanakubo, T. Makino, T. Umecky, CO<sub>2</sub> solubility in and physical properties for ionic liquid mixtures of 1-butyl-3-methylimidazolium acetate and 1-butyl-3-methylimidazolium bis(trifluoromethanesulfonyl)amide, J. Mol. Liq., 217 (2016) 112-119.
- [37] T. Makino, M. Kanakubo, Y. Masuda, T. Umecky, A. Suzuki, CO<sub>2</sub> absorption properties, densities, viscosities, and electrical conductivities of ethylimidazolium and 1-ethyl-3-methylimidazolium ionic liquids, Fluid Phase Equilib., 362 (2014) 300-306.
- [38] S. Seki, T. Kobayashi, Y. Kobayashi, K. Takei, H. Miyashiro, K. Hayamizu, S. Tsuzuki, T. Mitsugi, Y. Umebayashi, Effects of cation and anion on physical properties of room-temperature ionic liquids, J. Mol. Liq., 152 (2010) 9-13.
- [39] S. Kamalakannan, M. Prakash, G. Chambaud, M. Hochlaf, Adsorption of hydrophobic and hydrophilic ionic liquids at the Au(111) surface, ACS Omega, 3 (2018) 18039-18051.
- [40] D.A. Beattie, A. Arcifa, I. Delcheva, B.A. Le Cerf, S.V. MacWilliams, A. Rossi, M. Krasowska, Adsorption of ionic liquids onto silver studied by XPS, Colloids Surf. A Physicochem. Eng. Asp., 544 (2018) 78-85.

- [41] V. Lockett, R. Sedev, J. Ralston, M. Horne, T. Rodopoulos, Differential capacitance of the electrical double layer in imidazolium-based ionic liquids: Influence of potential, cation size, and temperature, J. Phys. Chem. C, 112 (2008) 7486-7495.
- [42] Z. Liu, T. Cui, T.Q. Lu, M.S. Ghazvini, F. Endres, Anion effects on the solid/ionic liquid interface and the electrodeposition of zinc, J. Phys. Chem. C, 120 (2016) 20224-20231.
- [43] C. Rodenbucher, K. Wippermann, C. Korte, Atomic force spectroscopy on ionic liquids, Applied Sciences-Basel, 9 (2019).
- [44] S.N.V.K. Aki, B.R. Mellein, E.M. Saurer, J.F. Brennecke, High-pressure phase behavior of carbon dioxide with imidazolium-based ionic liquids, J. Phys. Chem. B, 108 (2004) 20355-20365.
- [45] X. Zhang, L. Bai, S. Zeng, H. Gao, S. Zhang, M. Fan, Ionic liquids: advanced solvents for CO<sub>2</sub> capture, in: W.M. Budzianowski (Ed.) Energy efficient solvents for CO<sub>2</sub> capture by gasliquid absorption: compounds, blends and advanced solvent systems, Springer International Publishing, Cham, 2017, pp. 153-176.
- [46] J.L. Anthony, J.L. Anderson, E.J. Maginn, J.F. Brennecke, Anion effects on gas solubility in ionic liquids, J. Phys. Chem. B, 109 (2005) 6366-6374.
- [47] M.J. Muldoon, S.N.V.K. Aki, J.L. Anderson, J.K. Dixon, J.F. Brennecke, Improving carbon dioxide solubility in ionic liquids, J. Phys. Chem. B, 111 (2007) 9001-9009.
- [48] L. Cammarata, S.G. Kazarian, P.A. Salter, T. Welton, Molecular states of water in room temperature ionic liquids, Phys. Chem. Chem. Phys., 3 (2001) 5192-5200.
- [49] S.G. Kazarian, B.J. Briscoe, T. Welton, Combining ionic liquids and supercritical fluids: ATR-IR study of CO<sub>2</sub> dissolved in two ionic liquids at high pressures, Chem. Commun., (2000) 2047-2048.

- [50] B.L. Bhargava, S. Balasubramanian, Probing anion—carbon dioxide interactions in room temperature ionic liquids: Gas phase cluster calculations, Chem. Phys. Lett., 444 (2007) 242-246. [51] X.C. Zhang, Z.P. Liu, W.C. Wang, Screening of ionic liquids to capture CO<sub>2</sub> by COSMO-RS and experiments, Aiche Journal, 54 (2008) 2717-2728.
- [52] T. Seki, J.D. Grunwaldt, A. Baiker, In situ attenuated total reflection infrared spectroscopy of imidazolium-based room-temperature ionic liquids under "supercritical" CO<sub>2</sub>, J. Phys. Chem. B, 113 (2009) 114-122.
- [53] X. Zhang, X. Zhang, H. Dong, Z. Zhao, S. Zhang, Y. Huang, Carbon capture with ionic liquids: overview and progress, Energy Environ. Sci., 5 (2012) 6668-6681.
- [54] M. Besnard, M.I. Cabaco, F.V. Chavez, N. Pinaud, P.J. Sebastiao, J.A.P. Coutinho, J. Mascetti, Y. Danten, CO<sub>2</sub> in 1-butyl-3-methylimidazolium acetate. 2. NMR investigation of chemical reactions, J. Phys. Chem. A, 116 (2012) 4890-4901.
- [55] Q.B. Li, J.Y. Jiang, G.F. Li, W.C. Zhao, X.H. Zhao, T.C. Mu, The electrochemical stability of ionic liquids and deep eutectic solvents, Sci. China Chem., 59 (2016) 571-577.
- [56] Y. Hori, H. Konishi, T. Futamura, A. Murata, O. Koga, H. Sakurai, K. Oguma, Deactivation of copper electrode in electrochemical reduction of CO<sub>2</sub>, Electrochim. Acta, 50 (2005) 5354-5369.
- [57] D.V. Franco, L.M. Da Silva, W.F. Jardim, J.F.C. Boodts, Influence of the electrolyte composition on the kinetics of the oxygen evolution reaction and ozone production processes, J. Braz. Chem. Soc., 17 (2006) 746-757.
- [58] X.W. Zheng, S.T. Zhang, W.P. Li, M. Gong, L.L. Yin, Experimental and theoretical studies of two imidazolium-based ionic liquids as inhibitors for mild steel in sulfuric acid solution, Corros. Sci., 95 (2015) 168-179.

- [59] Basics of electrochemical impedance spectroscopy, Gamry Instruments, 2010.
- [60] H. Li, F. Endres, R. Atkin, Effect of alkyl chain length and anion species on the interfacial nanostructure of ionic liquids at the Au(111)–ionic liquid interface as a function of potential, Phys. Chem. Phys., 15 (2013) 14624-14633.
- [61] L. Cao, D. Raciti, C. Li, K.J.T. Livi, P.F. Rottmann, K.J. Hemker, T. Mueller, C. Wang, Mechanistic insights for low-overpotential electroreduction of CO<sub>2</sub> to CO on copper nanowires, ACS Catal., 7 (2017) 8578-8587.
- [62] D. Ren, J. Fong, B.S. Yeo, The effects of currents and potentials on the selectivities of copper toward carbon dioxide electroreduction, Nat. Commun., 9 (2018) 925.
- [63] M.B. Shiflett, A.M.S. Niehaus, B.A. Elliott, A. Yokozeki, Phase behavior of N<sub>2</sub>O and CO<sub>2</sub> in room-temperature ionic liquids [bmim][Tf<sub>2</sub>N], [bmim][BF<sub>4</sub>], [bmim][N(CN)<sub>2</sub>], [bmim][Ac], [eam][NO<sub>3</sub>], and [bmim][SCN], Int J Thermophys, 33 (2012) 412-436.
- [64] B. Ratschmeier, A. Kemna, B. Braunschweig, Role of H<sub>2</sub>O for CO<sub>2</sub> reduction reactions at platinum/electrolyte interfaces in imidazolium room-temperature ionic liquids,

  Chemelectrochem, 7 (2020) 1765-1774.
- [65] T. Kobayashi, A. Kemna, M. Fyta, B. Braunschweig, J. Smiatek, Aqueous mixtures of room-temperature ionic liquids: Entropy-driven accumulation of water molecules at interfaces, J. Phys. Chem. C, 123 (2019) 13795-13803.
- [66] L. Sun, G.K. Ramesha, P.V. Kamat, J.F. Brennecke, Switching the reaction course of electrochemical CO<sub>2</sub> reduction with ionic liquids, Langmuir, 30 (2014) 6302-6308.
- [67] R. Kortlever, J. Shen, K.J.P. Schouten, F. Calle-Vallejo, M.T.M. Koper, Catalysts and reaction pathways for the electrochemical reduction of carbon dioxide, J. Phys. Chem. Lett., 6 (2015) 4073-4082.